29 May 2010, 8:00 am - 9:30 am

Numerical and Experimental Investigation of Soil Behaviour Under Stationary Excitation

Holger Wienbroer
University of Karlsruhe (TH), Germany

Daniel Rebstock
University of Karlsruhe (TH), Germany

Gerhard Huber
University of Karlsruhe (TH), Germany


Fifth International Conference on
Recent Advances in Geotechnical Earthquake Engineering and Soil Dynamics
and Symposium in Honor of Professor I.M. Idriss
May 24-29, 2010 • San Diego, California

NUMERICAL AND EXPERIMENTAL INVESTIGATION OF SOIL BEHAVIOUR UNDER STATIONARY EXCITATION

Holger Wienbroer
University of Karlsruhe (TH)
Karlsruhe, Germany

Daniel Rebstock, Gerhard Huber
University of Karlsruhe (TH)
Karlsruhe, Germany

ABSTRACT

The effect of earthquakes on the behavior of soil and/or structures is usually investigated using earthquake-like signals as input for loading. This holds true for most of numerical and experimental simulations. In contrast to those approaches sinusoidal excitation was used here. The benefit of this type of excitation is an increased observability of the system, which is a precondition for a systematic investigation. Since sinusoidal excitation allows a gradually, step by step increase of the applied loading, the state of the soil (density and effective stress) as well as pore water pressure are transient. Therefore they are varying slowly and the modes of vibration are changing with time accordingly. The modes can be identified by regarding the contour of a soil column for instance. The evolution and distribution of pore water pressure (up to liquefaction) has to be captured simultaneously. A further advantage of this method is that asymptotic behavior can be investigated for the evolutions of pore water pressure and settlement of the surface with an increasing number of cycles.
On the base of a numerical study some test in a shake-box will be shown using the described concept. Numerical modeling of soil behavior under cyclic respectively dynamic loading requires the application of nonlinear constitutive laws. With the used FE-model it is possible to observe the dependence of excitation amplitude, frequency and initial state on the transient amplification of the sinusoidal input signal up to an onset of liquefaction. The appropriate experimental investigations confirm the numerically observed behavior. Therefore a shake-box under 1-g conditions with smooth boundaries is used for the tests. They were performed with a homogeneous soil column (about 0.8m length, 0.6m width, 2.1m height) from medium-grained quartz sand under saturated conditions.

INTRODUCTION

The type and state of soils near the surface (down to about 100m) have major influence on damages of structures build on them. It can be shown that waves propagating from the seismic source tend to propagate as horizontal shear waves towards the surface (Kramer, 1996). During real earthquakes most damages result from these shear waves. In many cases the soil behaviour near the surface is therefore considered in simulations as a 1-D-wave-propagation. This simplification is acceptable if the considered soil region is far away from the seismic energy source, then a periodic boundary condition is justified (cf. Fig. 1).
The non-linear nature of soil and effects like liquefaction and cyclic mobility require also non-linear constitutive relations. Such advanced constitutive relations for soil under earthquake like excitation have to be validated by laboratory tests. These laboratory tests can be performed by element like tests (cyclic triaxial tests, Resonant-Column tests), with 1g shake-box tests, or centrifuge tests at higher g-levels.

With cyclic triaxial tests it is not possible to reproduce shear-waves, as there is no rotation of the principal axes of strain. In Resonant-Column tests the specimen is normally brought to a resonance state. So real shear-wave propagation can only be investigated in shake-box tests. The commonly performed centrifuge tests at high g-levels have several disadvantages; however stress states like in-situ can be reproduced. This implies the use of scaling-laws which have to be fulfilled for all relevant parameters. Imagine a centrifuge test at 50g on a middle grained quartz sand (let's say d_{50} = 0.5mm) in model scale, this would give a gravel with d_{50} = 25mm in prototype scale. Additionally care has to be taken on the scaling of viscosity of the pore fluid, the stiffness of the boundary, etc... Therefore a different concept was chosen for the 1-g shake-box presented here. The test arrangement consists of a 1D-shake-table, a laminar shake-box attached and instrumentation with data acquisition.

For simulations linear or equivalent linear models (e.g. 'SHAKE' Schnabel et al., 1972) or similar programs are commonly used. If the state of soil is changing during an earthquake by a decrease of effective stress up to liquefaction, nonlinear and transient models including the stress/strain behaviour of the soil are required (Kramer, 1996; Iai and Tobita, 2006). Using nonlinear constitutive laws for 1-D wave propagation, measured and predicted accelerations for free-field conditions showed good agreement (Cudmani et al., 2003).

In order to model the dynamic behaviour in soft and liquefiable soils realistically, it is necessary to take the following essential aspects into account:

1. Non-linearity of the soil, development of excess pore water pressure and the associated reduction of effective pressure for undrained conditions,
2. hysteretic nature of soil damping,
3. radiation of wave-energy through the model boundaries (geometric damping), and
4. the state of soil as well as the base excitation signal applied to the subsoil.

The relevant mechanisms, the constitutive law being used, influence of state of soil and base excitation as well as experimental investigations will be considered in the following sections.

RELEVANT MECHANISMS

There are four mechanisms which have to be especially taken into account for a dynamic soil model: densification of soil, amplification of waves, decoupling of wave propagation in saturated soil, and liquefaction of soil. The phenomenon of soil liquefaction is one of the non-linear soil effects, which is most difficult to consider in the simulation. During strong earthquakes, liquefaction can cause large ground displacements which lead to devastating effects on structures as we know from many structural failures in past earthquakes. Most constitutive models available nowadays have not achieved yet the stage of development required to predict soil liquefaction reliably. The mentioned phenomena can be explained with the time history diagrams in Figure 1 (right).

First, an enlargement of amplitude (amplification) between the signal at depth and at the surface could be observed. This results from a decay in shear stiffness G due to a reduction of the effective mean pressure p'.

Second phenomena is that the the movement of the surface gets independent from the ground excitation with ongoing excitation (decoupling) Due to the cyclic shearing in the soil there is a gradual densification, also depending on the initial density, whereas under undrained conditions an increase in pore water pressure leads to a reduction of effective mean pressure p'. If the pore water pressure reaches the total mean pressure the grain skeleton disintegrates into a suspension, then we are talking about liquefaction. A liquefied zone is not able to transmit shear waves anymore, resulting in a decoupling.

An other effect of decoupling is based on hydraulic fracturing with the occurrence of water layers, cf. Kokushu, 2000. A compactable saturated soil sample under constant volume condition shows a water layer over the compacted grains skeleton after strong excitation. Such water layers can also occur due to earthquakes if a layer with low permeability is overlaying a compactable layer with higher permeability.

NUMERICAL INVESTIGATION

Constitutive Laws for Soil

The presented model allows examination of liquefaction and cyclic mobility for saturated soils. The subsoil behaviour is modelled with hypoplastic (Gudehus, 1996) and visco-hypoplastic constitutive equations (Niemunis, 2003) which are able to simulate the response of cohesionless and cohesive soils under monotonous loading. The extension of the constitutive relation by the concept of intergranular strain enables a realistic alternating loading. In contrast to elastoplastic models the used hypoplastic description distinguishes between material parameters and state variables. The material parameters are: the so-called granulate hardness h_s and the exponent n describing the compressibility of the grain skeleton, the critical state friction angle φ_c , the characteristic void ratios e_{d0} (lowest), e_{c0} (critical) and e_{i0}

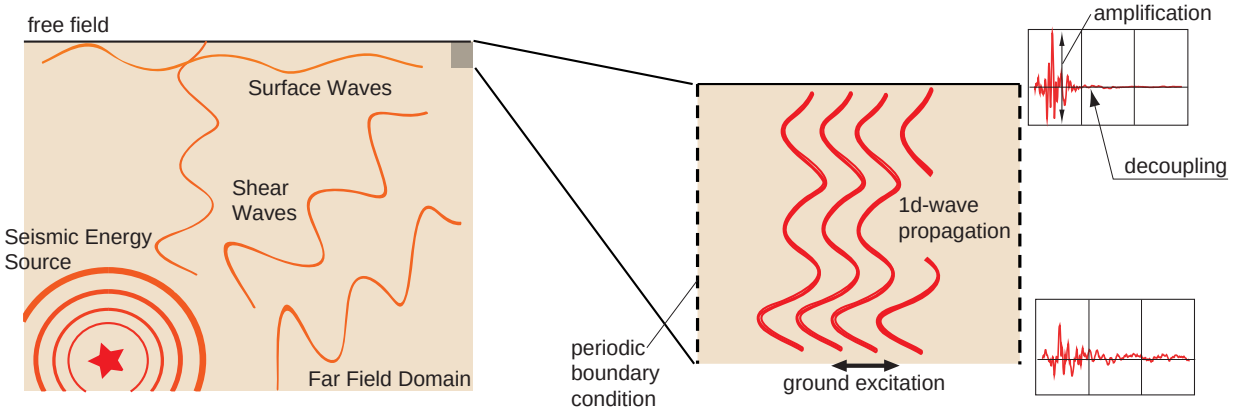

Fig. 1. Principle scheme of the wave propagation.

(highest) at zero pressure (Index 0) and the exponents α and β controlling the density influence on peak friction angle and compressibility (Table 1).

These material laws are used to model plastic deformations of grain skeletons incorporating the critical state concept of soil mechanics. Strength and stiffness depend on current stress state σ, density (via void ratio e), deformation rate $\dot{\varepsilon}$ and deformation history δ. Subsequently commonly used parameters such as shear modulus G, damping D and velocity of propagation c are state dependent, and do not have to be known in advance as with other constitutive relations.

h_s [MPa]	4000
n	0.25
e_{d0}	0.55
e_{c0}	0.95
e_{i0}	1.05
φ_c [°]	32.1
α	0.07
β	1.0

Table 1. Hypoplastic soil parameters (quartz sand).

The total mean stress p is separated in the constitutive law into effective stress p' and pore water pressure p_w: $p = p' + p_w$. The mechanical behaviour of soil is governed by effective stress p'.

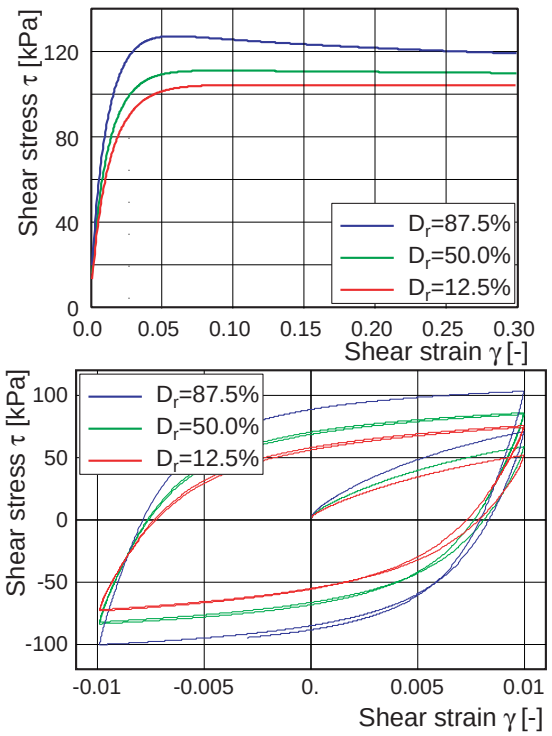

Fig. 2. Calculated simple-shear test: monotonic (top) and cyclic (bottom); shear-stress τ vs. shear-strain γ for different relative density (quartz sand).

In case of undrained deformation, the evolution of the pore water pressure p_w depends on volumetric deformation taking into account the bulk modulus of the water k_w.

Stationary results for a simulated monotonous and cyclic simple-shear-test are shown in Figure 2 and 3 for K_0-state with mean pressure $p' = 100$ kPa. The cyclic tests were performed with a shear-strain amplitude γ up to 1%. The influence of relative density D_r is visible for dense ($D_r = 87.5\%$; $e_0 = 0.60$), medium ($D_r = 50\%$, $e_0 = 0.75$) and loose ($D_r = 12.5\%$, $e_0 = 0.90$) sand. The relative densities are calculated after the common relation with the initial void ratio e_0 and the limit void ratios e_{max} ($e_{c0} \approx e_{max} = 0.95$) and e_{min} ($e_{d0} \approx e_{min} = 0.55$) according to the German standard DIN 18126.

$$D_r = \frac{e_{max} - e_0}{e_{max} - e_{min}} \qquad (1)$$

The decay of equivalent shear-modulus G and simultaneous increase of damping ratio D for shear-strain amplitude $\gamma > 10^{-4}$ arises similarly to measurements of resonant-column tests, ref. Figure 3 (top).

The equivalent shear-modulus G_0 for small shear-strain amplitudes γ_0 dependending on effective mean pressure p' is shown in Figure 3 (bottom). The velocity of propagation of shear-waves c_s can be easily calculated in dependence of depth with known density of saturated soil ρ_{soil} (≈ 2.1 to/m³), cf. Figure 4.

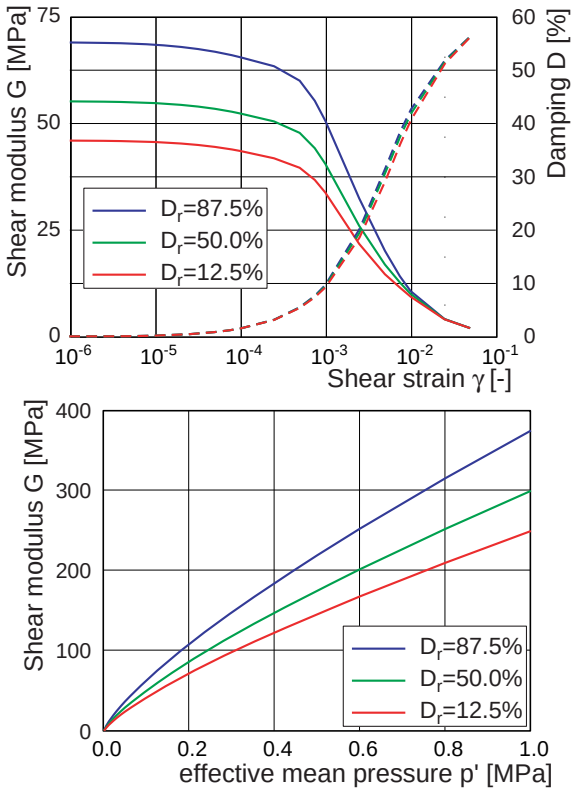

Fig. 3. Calculated equivalent shear-modulus G and damping ratio D vs. shear-strain amplitude γ (top) and G_0 vs. effective mean pressure p' for small shear-strain amplitude γ (bottom) for different relative density (quartz sand).

$$c_s = \sqrt{G / \rho_{soil}} \qquad (2)$$

with

$$p' = \frac{1 + 2 \cdot K_0}{3} \cdot \left(\rho_{soil} - \rho_{water}\right) \cdot g \cdot z \qquad (3)$$

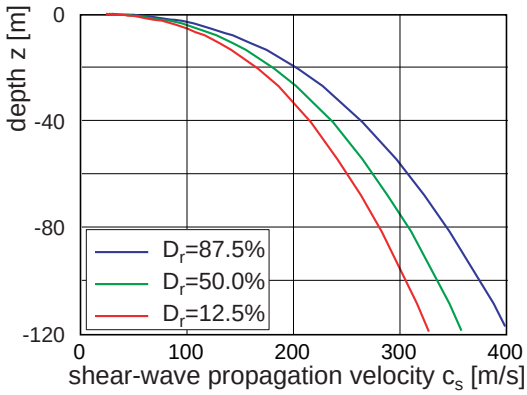

Fig. 4. Shear-wave propagation velocity vs. depth (bottom) for different relative density (quartz sand).

Wave-Propagation for Free-Field Condition

Nonlinear effects were considered with transient wave propagation from an originally homogeneous soil column for free-field conditions including liquefaction in a quasi one dimensional problem. Sinusoidal signals are more convenient for systematic investigations because earthquake signals contain rapidly changing velocity amplitudes and frequency content (Figure 1):

- observability is enabled due to slowly varying states of soil while increasing the sinusoidal (monofrequent) excitation moderately;
- advantages of stationary excitation are identification of modes of vibration, asymptotic behaviour (attractors) depending on amplitude as well as on frequency. Due to nonlinearity the modes of vibration are also varying with time;
- residual states can be achieved, which is essential for an evaluation of nonlinear constitutive laws reaching an asymptotic behaviour (attractors) and/or state limits.

In a parametric study the transient behaviour of a saturated soil column under sinusoidal excitation shows amplification and reduction of surface vibrations depending on excitation amplitude, frequency, number of cycles and density of soil. Certainly, these effects also appear with an earthquake signal, but a separation into the mentioned parameters of excitation is not cumbersome.
The presented calculations are based on continuummechanics as they were accomplished with FEM in order to check other methods. The full 3D-formulation of the dynamic calculation is a further advantage of the used FE-Code ABAQUS.

FE-Model. The simulations presented were accomplished with the FE-Code ABAQUS 6.5. The FE-model of the soil-column consists of 240 elements (Figure 5 left). An implicit time-integration is used for the dynamic calculations. During the earthquake, water drainage is not permitted, i.e. undrained soil behaviour is assumed. A lateral periodic boundary condition of the soil is imposed by constraining opposite nodes on these boundaries to undergo the same displacement. This boundary condition is reasonable for strong earthquakes since the energy dissipation in the soil due to (hysteretic) damping supersedes the energy radiation from the foundation. The periodic boundary condition provides exact results in the case of level ground with free surface subjected to base shaking without structure (Gudehus et al., 2004). The parameters for variation with sinusoidal bedrock excitation at the bottom nodes of the model are velocity-amplitude and frequency.

Reference Example. As reference simulation the following properties were applied: Frequency f = 2 Hz, excitation

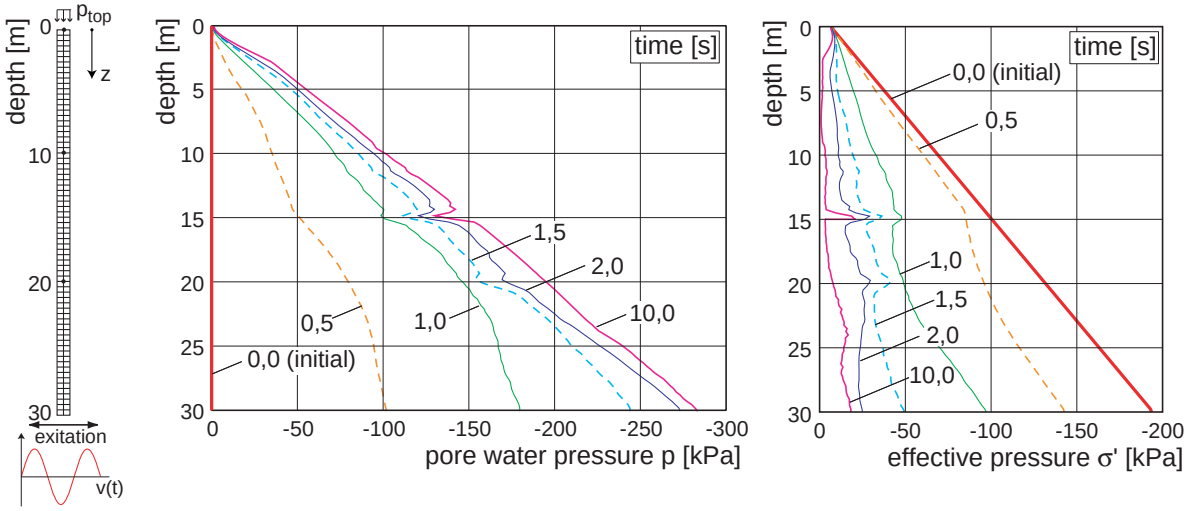

Fig. 5. Pore water pressure (left) and effective stress (right) at different times.

amplitude v_{bottom} = 0.4 m/s, height of soil column h = 30 m (Material parameters cf. Table 1) and relative density D_r = 50% (medium dense, e_0 = 0.7). On top of model an extra load of p_{top} = 10 kPa is applied because of numerical stability requirements. Results are evolution of excess pore water pressure and mean effective pressure for different time steps (Figure 5 middle). Beginning at the bottom, p_w increases and simultaneously p' decays rapidly. After about two seconds the effective pressures (Figure 5 right) almost vanish, i.e. the stiffness of the layer is strongly reduced (onset of liquefaction).

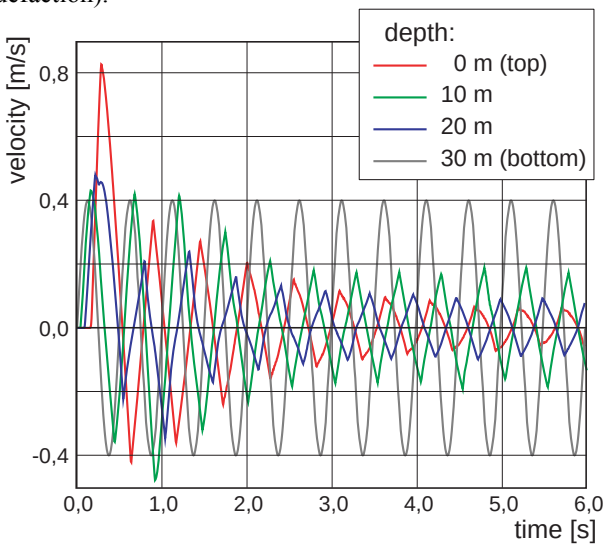

Fig. 6. Velocity time history at different depths.

The wave propagation is shown in Figure 6 with horizontal component of velocity at different depths. Caused by the change of stiffness from bottom to top shear wave velocity decreases and thus amplitude will increase. The transient reduction of the amplitude caused by reduction of stiffness after an initial amplification is clearly shown. As the calculations are performed under undrained condition settlements after consolidation have to be estimated by the change in void ratio.

Transient mode of vibration. The amplification is the relation between horizontal velocity amplitude of ground excitation v_0 and horizontal velocity of surface point $v(t)$ in calculation:

$$\text{amplification} = \frac{|v(t)|}{v_0} \qquad (4)$$

The maximum value is reached during the first cycles, and after a sufficient number of cycles the residual amplitude arises. The amplification vs. time for v = 5 cm/s is plotted as time-history (dotted) and the envelop (line) in Figure 7. In this case, the change of amplification and mode of oscillation in time is obvious. For particular times t with maximum deflection (4.00/4.25 s, 14.00/14.25 s, 20.75/21.00 s) the displacement contour of the column vs. depth is shown. The first mode similar to $\lambda/2$ is visible in a), b) and c) show higher modes (with λ = wavelength for "natural" frequency).

Variation of excitation. In a first study the velocity amplitude v of ground excitation was varied between 5 and 80 cm/s. Figure 8 compares the amplification using the envelops for different excitation amplitudes. The significant amplification (maximum value) for low velocities in contrast to higher velocities is remarkable. For higher velocities the amplification to a residual value decays even faster. This is caused by the more rapid reduction of stiffness resulting from lower effective pressure and size of shear-strain amplitude caused by dynamic effects.

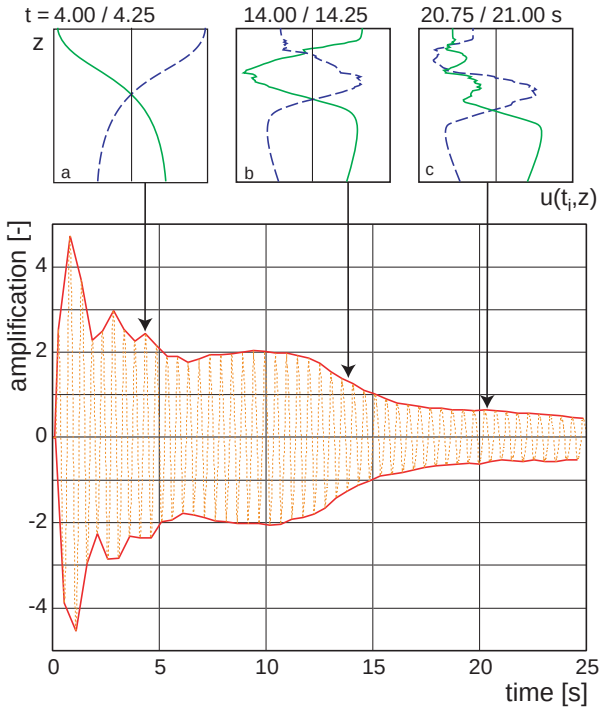

Fig. 7. Change in amplification vs. time for v = 5 cm/s and f = 2 Hz (bottom) and transient change of vibration mode at particular times (a, b, c) (top).

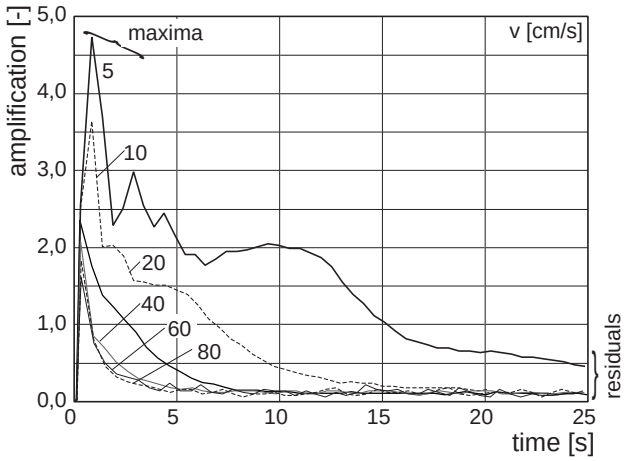

Fig. 8. Envelopes for different base velocity amplitudes v for constant frequency f = 2 Hz.

As mentioned above, the second varied parameter is frequency. Figure 9 depicts the amplification for two different velocity amplitudes. Starting with rigid body motion at very

low frequencies amplification of approximately one occurs. With increasing frequencies a pseudo resonance peak will be achieved for the first few cycles. This amplification suggests a "natural" frequency of about 1.6 Hz for the examined soil column.

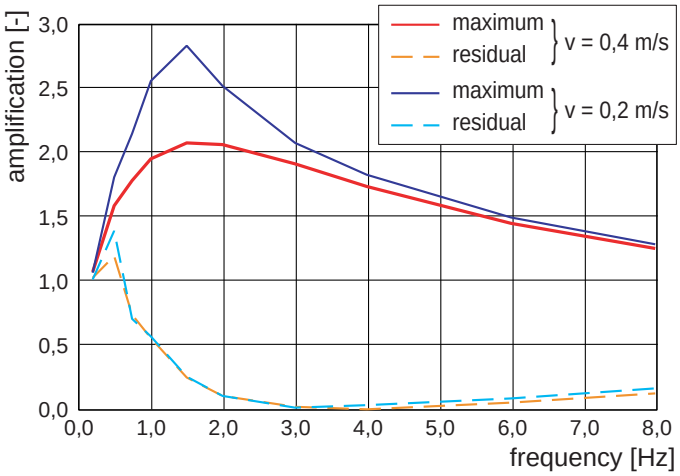

Fig. 9. Variation of ground excitation – amplification vs. frequency for two velocities.

After a sufficient number of cycles at higher frequencies the residual amplitudes are strongly reduced (amplification << 1) independent of excitation velocity. This is caused by onset of liquefaction. For lower frequencies there is still a resonance like local maximum for residual amplification at approx. 0.5 Hz due to the elastic range in the constitutive law. In contrast to the maximum curve this curve is shifted to lower frequencies. The change in resonance frequencies and amplifications is due to the nonlinearity of soil. For small amplitudes and very low frequencies (< 0.25 Hz) the motion of the column is to be assumed as a rigid body (amplification = 1) due to negligible inertia.

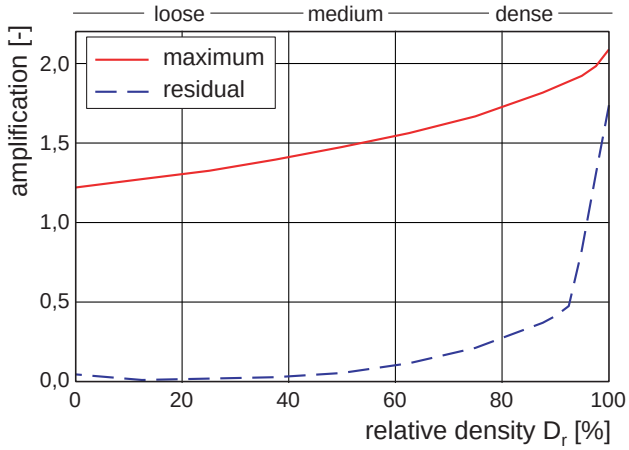

Fig. 10. Variation of density; amplification vs. initial void ratio for v = 0,4 m/s and f = 2 Hz.

Variation of density. Figure 10 shows the influence of initial relative density. There is a decay of the maximum amplification for decreasing relative density. Medium dense sand has only in first few cycles this amplification. Cyclic shearing leads to densification, and thus to an increase of pore water pressure. After few cycles there is a decoupling for initial relative density lower than 50%. For dense sand negative pore water pressure occurs due to inability of further densification of soil. This results in significant remaining amplification.

EXPERIMENTAL INVESTIGATION

Experimental setup

The tests presented here refer to so-called shakebox tests at 1g with a new smooth boundary condition due to pivoted frames. The test arrangement consists of a 1D-shake-table, a laminar shake-box and instrumentation with data acquisition (Figure 11 left).

Shake table. The shake-table uses a one-dimensional closed loop servo-controlled hydraulic drive which generates the excitation movement for the shake-box. It can be freely chosen whether a harmonic (sinusoidal) signal from a wave generator is used or a random or earthquake like signal is imposed. The signals have only to stay within certain limits to avoid amplitude reduction and phase shift of movement (Table 2). The advantage of sinusoidal signals is in the possibility of a systematic investigation of the influence of amplitude, frequency and number of cycles.

f [Hz]	limit	
< 0.3	$u_0 \leq 120$ mm	cylinder stroke
0.3 - 10	$v_0 \leq 0.19$ m/s	oil flow rate
10 - 30	$a_0 \leq 1.1$ g	hydraulic pressure

Table 2. Operating capacity of shake-table.

Laminar shake-box. In order to avoid the difficulties with scaling laws the following concept was applied. For the validation of constitutive models (e.g. hypoplasticity) it is not necessary to bring a prototype case to model scale via scaling laws. Therefore it is only needed to have a well defined experimental setup for a simulation. This means that the state of the soil (stress state and void ratio) and the boundary conditions have to be known at the beginning and for any time during the test. The changes have to be within the measurable range and resolution of the transducers.
The most important geometrical value to achieve this is the height of the box, it determines the mean pres-sure and possible modes of vibration. To observe wave propagation a major part of the wavelength must fit into the column. For technical reasons (total soil mass, functional location structure, feasibility) the shake-box height is limited to about two meters. There is only a minor influence of length and width of the box to the vibration behavior.
From a practical point of view the length in the direction of movement is 80 cm and perpendicular the width is 60 cm (soil

volume: 1 m³). The mass of the specimen with a height of h = 2.1 m is about 1500 kg for medium dense dry sand. For tests with fine-grained material like silt and clay it is not feasible to fill the full setup to a defined state. In this case the height of the box can be reduced to one third (h = 0.7 m).
Care has to be taken also on smooth boundaries in the deflected direction of the box, which should not constrain the wave propagation. Ordinary shake-boxes are equipped with a stack of frames with rigid walls supporting the soil sample. This setup might be feasible for centrifuge tests with small differential movement of the frames. If the movements get too big one gets locally larger shear deformations at the connections of frames than in the remaining soil body. In order to reduce the influence of these fixed walls of each frame, two oppositely placed walls (perpendicular to direction of excitation) of frames are allowed to rotate. This leads to a rather smooth boundary (Figure 11 right).
The "shear stiffness" of the frame structure is normally assumed to be the same as the soil stiffness – this approach is often used in centrifuge tests. As we want to observe a large variation of soil stiffness up to liquefaction the "shear stiffness" and inertia of the pivoted frames is minimized. This implies also that the dead load of the frames has to be compensated, which is done via four soft springs. To minimize the influence of mass of the frames on the oscillation properties of the system their mass is reduced to below 20% of the soil mass per frame. For the whole setup with 2.1 m height the construction consists of 24 frames, or 8 frames for the small setup. The soil sample inside the shake-box is surrounded by a water-proof rubber membrane.

Measurement equipment. The horizontal deflection of each frame or lamella is measured by displacement transducers (DT 1-24). The transducer bodies are mounted on a fixed measurement rig. The sliders are connected to the frames. An additional transducer (DT table) is connected to the moving table. Relative displacements have to be calculated from the recorded data. The measurement range of the transducers is 300 mm with a resolution of 30 µm. A direct relative measurement from frame to frame is not feasible because of the transducer size and the wiring. All other quantities like velocity, acceleration and strain have to be derived from the measured displacements. Conventional piezo-electric acceleration transducers could capture the relative values directly, but at low frequencies they are inappropriate. Geophones are also not applicable for similar reasons.
The development of excess pore water pressures inside the specimen is measured in four different heights with four pore pressure transducers (PPT). The measurement range of these relative pressure transducers is 0 - 40 kPa. The transducers are mounted outside the box and connected to the pore fluid via stainless steel tubes (outer diameter 4 mm, inner diameter 2 mm). The tubes end at heights of z = 0.0, 0.4, 0.8 and 1.2 m. The upper ends are equipped with small filter stones. The density of the fluid or the fluidized soil above the filter stone dictates the measured pressure. All tubes are installed perpendicularly to the direction of movement to avoid pressure changes due to inertial forces of the water in the tubes. Advantages of this arrangement are the ensured absence of air in the measurement system, no subsidence or ascension of the transducers during testing, and all transducers show the same pore water pressure as they are mounted at the same geodetic height. Lateral infiltration along the cables as it may occur with immersed transducers is avoided.
The settlement of the soil column is measured with two separate systems. Two laser displacement meters (LDM) with

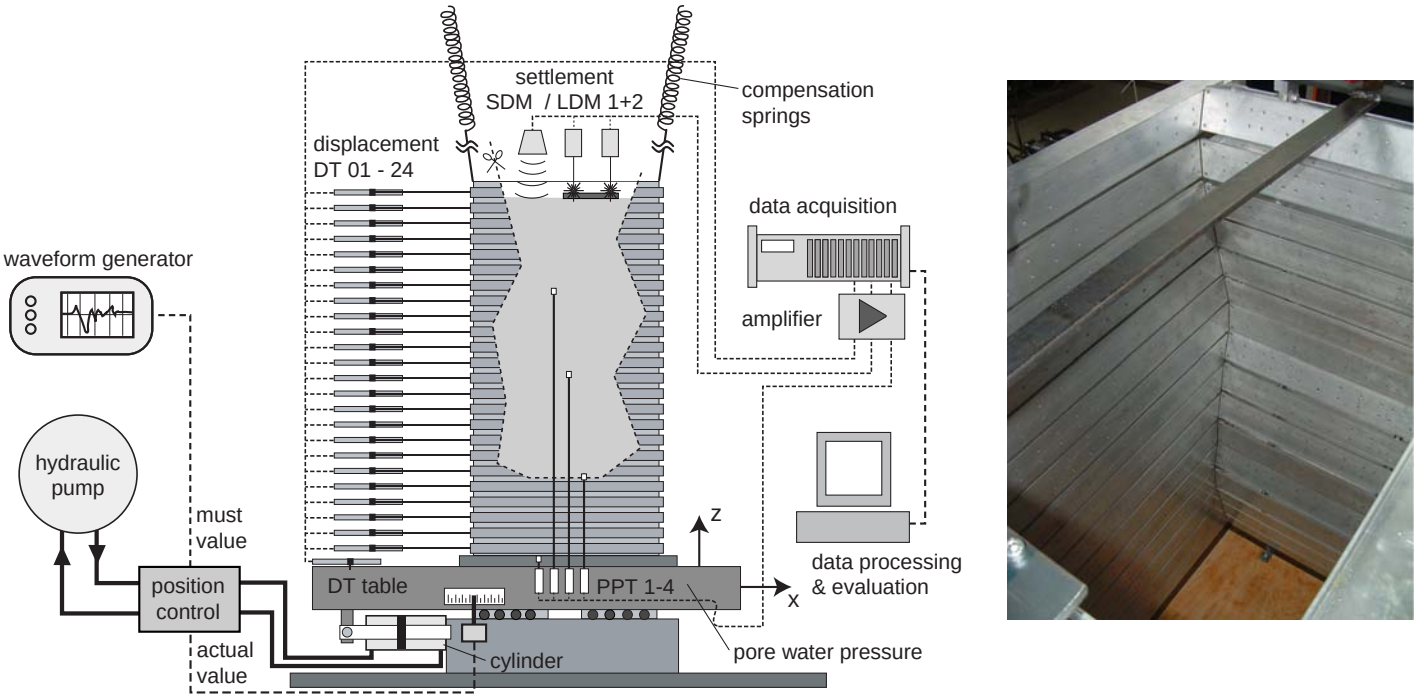

Fig. 11. Scheme of experimental setup with shake-table, laminar shake-box and measurement equipment (left), inside view of deflectedframes (right).

50 mm measurement range and 10 µm resolution allow the continuous registration of the surface settlement and the identification of rocking modes. These LDMs acquire the distance between the LDM and a small elevated target plate placed on the soil surface. Large settlements can exceed the measurement range, or in the case of liquefaction the target plate sinks, in both cases the in-formation about the settlement during one tests gets lost. An additional non-contact ultra-sonic displacement meter (SDM) with a measurement range of 240 mm and resolution of 1 mm is used. It allows the registration of the total settlement of the soil or water surface during all series of tests. Measuring the height of the soil column requires the extraction of water from the soil surface after each test. The combination of LDM and SDM assures a good global and local accuracy for the displacement of the soil surface.

The data acquisition is done simultaneously for all transducers with a sampling rate of 600 Hz. Anti-aliasing filters (40 Hz and Bessel type) with constant group delay serve to avoid dispersion.

Shake-box tests

Material and sample preparation. The material used in the tests was "Karlsruhe Sand" which is an artificial sand-mixture with a mineralogical composition of 82% quartz, 15% feldspar and 3% calcite. The grain shape of the medium grained sand with $d_{50} = 0.60$ mm can be characterised as subangluar. The limit void ratios are $e_{min} = 0.578$ and $e_{max} = 0.858$ according to the German standard DIN 18126. The critical friction angle is $\varphi_c = 30.1°$.

To prepare a sample of saturated sand, the box first has to be fixed in the upright position by a supporting construction (pivoted lamellas vertical). Then it is filled with water up to about 1.9 m - the tubes for the pore pressure measurement were in-stalled and de-aerated before. The sand is pluviated on the water surface from a sieve box which is filled from a container. The sieve box is moved back and forth during emptying the container evenly, to achieve a relatively plane sand surface below the water. The sand is brought in with 6 strokes (total mass of dry sand: 1500 kg). During this procedure the water level was kept constant (surplus water was sucked off with vacuum support), so only the sedimentation depth varies from 2.0 to 0.0 m. Disadvantage of this method is a light decomposition of the sand during the sedimentation process. At the end the soil surface is planated, the compensation springs are installed and the supporting construction can be removed. Medium dense samples could be achieved with this installation procedure.

Liquefaction test. All tests were performed using a harmonic (sinusoidal) excitation signal with a frequency of 1 Hz. The test series started with an amplitude $u_0 = 5$ mm. 50 cycles were performed with this amplitude and repeated 3 times, then the amplitude was increased to $u_0 = 10$ mm. Fifty cycles were

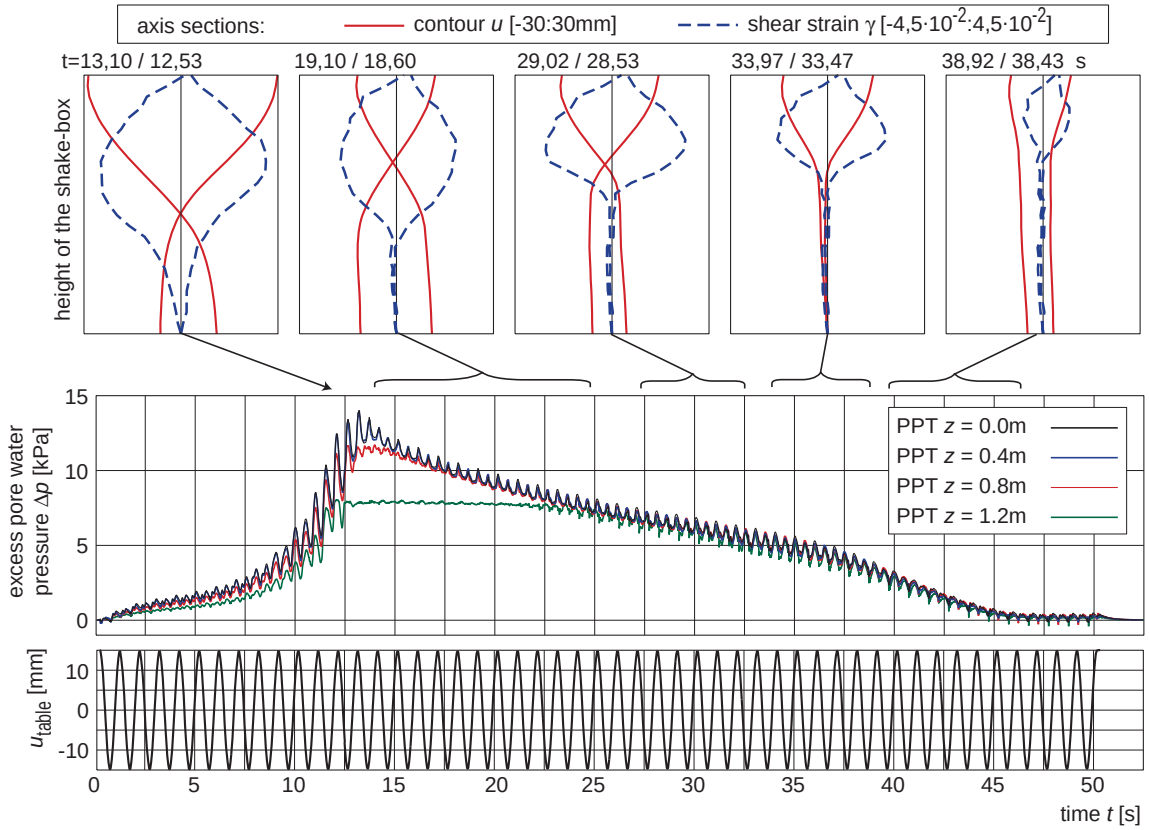

Fig. 13. Excitation u_{table} and pore water pressure Δp for different depth during liquefaction and reconsolidation (bottom). Contour u and shear strain distribution γ over height at different times (top)

chosen to have a sufficient number of cycles to reach stationary behavior. A three fold repetition was done in order to reach an almost stationary state for the same excitation. During the first two amplitudes settlements $\Delta s = 7$ mm were measured (Figure 12). The settlement rate decreases and the pore water pressure build up of about $\Delta p = 1$ kPa gets smaller from test to test.

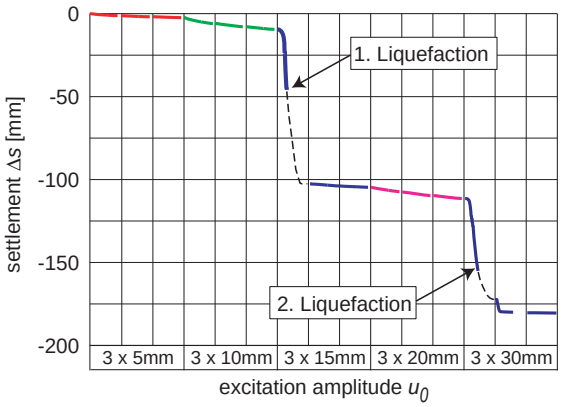

Fig. 12. Settlement Δs vs. excitation amplitude u_0 of the test series.

The presented test of the third series shows a quite different behavior (Figure 13). The amplitude was increased to $u_0 = 15$ mm ($v_0 = 94.2$ mm/s), and after 12 sec the upper part of the soil column liquefies (about $z = 0.8$ m above base level). Subsequently the excess pore water pressure decays from bottom to top, i.e. the soil reconsolidates. After 22 sec the last PPT ($z = 1.2$ m) is reached. The hydrostatic static is attained at about 45 seconds.

During the test a settlement $\Delta s = 93$ mm was measured. With the initial height of the soil column (before liquefaction) of $h = 1.975$ m and the settlement, the mean void ratios before and after the test can be estimated. Expressed in relative densities $I_D = (e_{max} - e) / (e_{max} - e_{min})$ this results in a densification from $I_D = 49\%$ to 77%.

From the pore pressure measurements the effective stress at the filter-stone level can be estimated, assuming undrained conditions. Using the initial void ratio $e = 0.643$ ($I_D = 49\%$) a mean effective unit weight of $\gamma' = 9.74$ kN/m³ can be calculated, and an approximate effective stress σ' at the PPT levels can be estimated (neglecting the density distribution vs. height). In Figure 14 the pore water pressure p in-creases until the total stress line is reached. With the principle of effective stress $\sigma' = \sigma - p$ it follows that the effective stress σ' vanishes, so the soil is liquefied. Liquefaction occurs approximately above $z = 0.8$ m.

The contour of the shake-box and the derived shear strains over the height for different times (the times of maximum shift between table and upper-most frame were chosen) are shown in Figure 6 (top). In each case the ranges are marked for which the plotted mode is representative. In the first 15 seconds the shear strain increases evenly over the box height. For the moment of liquefaction (12 sec) the maximum shear deformation arises (up to $\gamma = 4.5\%$) in the centre of the box.

The on-going reconsolidation from bottom to top after liquefaction can be seen in the maximum in shear strain moving upward. Simultaneously the pore pressure decreases gradually. This changes stiffness and wavelength as well as the mode of vibration. From 12 to 30 sec the upper part of the box moves in opposite phase referred to the table. After 40 sec the whole box moves in phase. Reconsolidation ends at 45 sec and rigid body movement follows with very small shear strain. Further tests with stepwise increased amplitude were performed. Due to the stronger excitation ($u_0 = 30$ mm) liquefaction could again be achieved with larger shear deformations (up to 10%), cf. Wienbroer et. al., 2007.

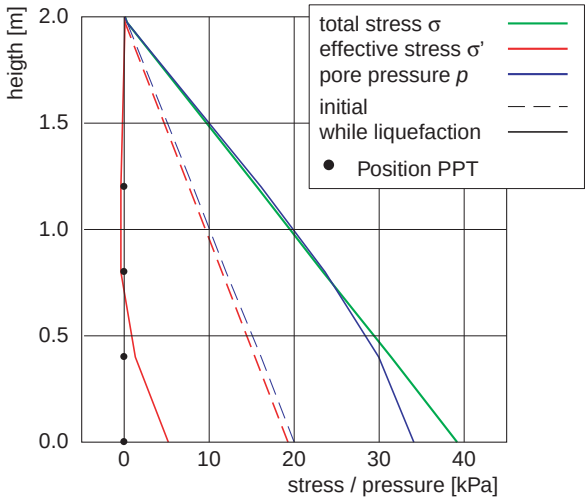

Fig. 14. Stress and pore pressure distribution for initial state and during liquefaction.

CONCLUSIONS

There are several effects in soil near the surface observed from experiments and during earthquakes. They result from nonlinear behavior and lead to a transient change of the state of the soil, increasing pore water pressure thus decreasing effective stress up to liquefaction.

It is not necessary to prescribe a shear strain dependent shear modulus like in linear or semi-linear wave propagation models, if a nonlinear hypoplastic constitutive relation is used. Only conventional properties of soil and its state are needed for this constitutive relation. Considering a homogenous soil column (e.g. without layers) allows a comparably easy interpretation of the results and shows the major mechanisms of the initial boundary value problem.

Reliable measurements of pore water pressure with no obvious lateral infiltration were achieved in the shake-box tests. Cyclic mobility was identified by transient pore water pressure changes at comparably small displacements and inhomogeneous pressure distribution over the height of the sample. Phases with very low effective stress and nearly constant pore water pressure could be observed. This means that liquefaction and reconsolidation could clearly be identified.

The periodic excitation enables an insight in the transient behavior of soil. Thus it is possible to identify slowly varying modes of vibration, which holds true for numerical calculations and experiments. For the experiments a careful choice and a moderate increase of excitation are essential to obtain observable slowly varying stages. The tests performed show the ability to achieve this behavior. This implies that the basic requirements for a numerical simulation are given.
Dynamic numerical simulations of the tests considering all effects require a model including consolidation and seepage. Until now the emission of water or flow of water cannot be simulated with available constitutive models. Usually only fully drained or undrained conditions can be simulated, but only minor stages of the test comply to these conditions. The observed transient changes in the modes of vibration have been simulated for undrained conditions.
The numerically and experimentally gained results show a qualitatively good analogy in the change of vibration mode and porewaterpressure buildt-up for the stages with undrained conditions. A variation of excitation amplitude and frequency obviously leads to a change of amplification which is connected to the liquefaction behavior. Most of the variations were done numerically because the experiments are very time consuming.

ACKNOWLEDGEMENTS

The research for the presented work was supported by the Deutsche Forschungsgemeinschaft (DFG) in the scope of the Collaborative Research Centre (CRC 461) "Strong Earthquakes: A Challenge for Geosciences and Civil Engineering".

REFERENCES

Cudmani R., V. Osinov, M. Buehler and G. Gudehus [2003]. "A model for evaluation of liquefaction susceptibility in layered soils due to earthquakes", *Proc. 12th Pan-American Conference on SMGE*, Cambridge, Vol. 2, pp. 969–976.

DIN 18126 [1996]. *"Bestimmung der Dichte nichtbindiger Böden bei lockerster und dichtester Lagerung"*, Normenausschuss Bauwesen im Deutschen Institut für Normung e. V..

Gudehus G. [1996]. "A comprehensive constitutive equation for granular materials", Soils and Foundations, No. 36(1), pp. 1-12.

Gudehus G., R. Cudmani, A. Libreros-Bertini and M. Buehler [2004]. "Inplane and anti-plane strong shaking of soil systems and structures", Soil Dynamics and Earthquake Engineering, No. 24, pp. 319–342.

Iai S. and T. Tobita [2006]. "Soil non-linearity and effects on seismic site response", *Proc. 3rd Symposium on the Effects of Surface Geology on Seismic Motion*, Grenoble, KN2, pp. 21-46.

Kokusho, T. [2008]. "Water film in liquefied sand and its effect on lateral spread", J. Geotech Engrg, ASCE, 125(10), pp. 817-826.

Kramer S.L. [1996]. *"Geotechnical Earthquake Engineering"*, Prentice-Hall International Series in Civil Engineering and Engineering Mechanics, Prentice Hall, New Jersey.

Niemunis A. [2003]. *"Extended hypoplastic models for soils"*, Habilitation-Thesis, University Bochum, No. 34.

Schnabel B., J. Lysmer and H.B. Seed [1972]. "SHAKE – a computer program for earthquake response analysis of horizontally layered sites", Report EERC, No. 72-12.

Wienbroer, H., D. Rebstock, and G. Huber [2007]. "Shake-Box Tests" *Proc. International Symphosium on Strong Vrancea Earthquakes and Risk Mitigation*, Bucharest, pp. 226-239.